Article

Chemistry & Biology

Metabolic Regulation of Histone Acetyltransferases by Endogenous Acyl-CoA Cofactors

Graphical Abstract

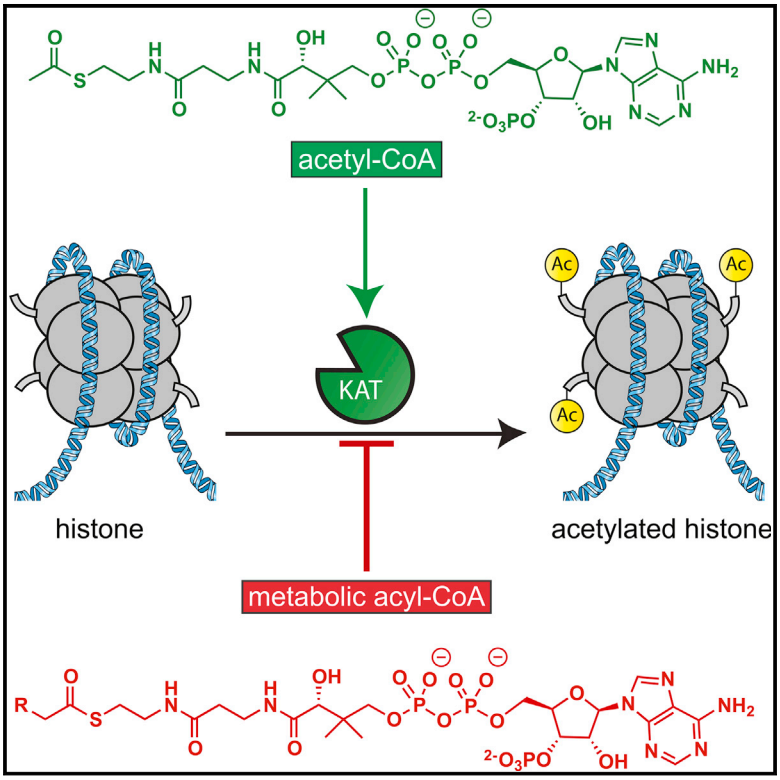

Highlights

- A new chemoproteomic probe enables the study of endogenous KAT complexes
- Palmitoyl-CoA impedes active site dependent enrichment of cellular KATs
- Fatty acyl-CoAs are potent competitive inhibitors of Gcn5-catalyzed acetylation
- Fatty acyl-CoA precursors reduce cellular acetylation

Authors

David C. Montgomery, Alexander W. Sorum, Laura Guasch, Marc C. Nicklaus, Jordan L. Meier

Correspondence

jordan.meier@nih.gov

In Brief

Montgomery et al. describe the application of a chemoproteomic approach to identify metabolic inhibitors of KAT enzymes. They find that long fatty acyl-CoAs strongly antagonize KAT activity, and that fatty acyl-CoA precursors reduce histone acetylation in cells.

Montgomery et al., 2015, Chemistry & Biology 22, 1030–1039
August 20, 2015
http://dx.doi.org/10.1016/j.chembiol.2015.06.015

CellPress

CellPress

Chemistry & Biology
Article

Metabolic Regulation of Histone Acetyltransferases by Endogenous Acyl-CoA Cofactors

David C. Montgomery,[1,2] Alexander W. Sorum,[1,2] Laura Guasch,[1] Marc C. Nicklaus,[1] and Jordan L. Meier[1,*]
[1]Chemical Biology Laboratory, Center for Cancer Research, National Cancer Institute, National Institutes of Health, Frederick, MD 21702, USA
[2]Co-first author
*Correspondence: jordan.meier@nih.gov
http://dx.doi.org/10.1016/j.chembiol.2015.06.015

SUMMARY

The finding that chromatin modifications are sensitive to changes in cellular cofactor levels potentially links altered tumor cell metabolism and gene expression. However, the specific enzymes and metabolites that connect these two processes remain obscure. Characterizing these metabolic-epigenetic axes is critical to understanding how metabolism supports signaling in cancer, and developing therapeutic strategies to disrupt this process. Here, we describe a chemical approach to define the metabolic regulation of lysine acetyltransferase (KAT) enzymes. Using a novel chemoproteomic probe, we identify a previously unreported interaction between palmitoyl coenzyme A (palmitoyl-CoA) and KAT enzymes. Further analysis reveals that palmitoyl-CoA is a potent inhibitor of KAT activity and that fatty acyl-CoA precursors reduce cellular histone acetylation levels. These studies implicate fatty acyl-CoAs as endogenous regulators of histone acetylation, and suggest novel strategies for the investigation and metabolic modulation of epigenetic signaling.

INTRODUCTION

Lysine acetylation plays a critical role in regulating chromatin structure. By neutralizing the positive charge of histone tails, acetylation serves to relax histone-DNA interactions and allows *trans*-acting factors to access genomic chromatin (Roth et al., 2001). Lysine acetylation also provides binding sites for effector proteins known as bromodomains, which can directly stimulate transcription by recruiting coactivators (Dhalluin et al., 1999). Global reductions in histone acetylation are correlated with aggressive disease and poor clinical outcome in many cancers (Seligson et al., 2005, 2009), and small molecules that counteract this profile and restore acetylation are validated therapeutic agents (Marks and Breslow, 2007). Defining the cellular mechanisms that regulate acetylation is thus of critical importance to understanding the biology of cancer and developing novel strategies to combat disease.

Protein acetylation is established by the opposing functions of lysine acetyltransferase (KAT) and lysine deacetylase (KDAC) enzymes. In addition to their role in transcription, the activity of these enzymes appears to be intimately linked to the metabolic state of the cell (Meier, 2013). For example, KDAC activity can be modulated by endogenous inhibitors such as diet-derived short-chain fatty acids and ketone bodies (Donohoe et al., 2012; Shimazu et al., 2013). By comparison, less is known about the metabolic mechanisms that influence KAT activity. Disrupting production of the KAT cofactor acetyl coenzyme A (acetyl-CoA) has been shown to inhibit histone acetylation (Comerford et al., 2014; Wellen et al., 2009). However, since all characterized human KATs exhibit Michaelis constants for acetyl-CoA far below its estimated cellular concentration (Tanner et al., 2000a; Thompson et al., 2001), it has been proposed that rather than becoming inherently rate limiting, low acetyl-CoA levels make KATs more susceptible to inhibition by CoA, an endogenous feedback inhibitor (Albaugh et al., 2011; Lee et al., 2014). Evidence from biochemical analyses and studies in yeast suggest that the GCN5 family of KATs may be particularly susceptible to this mechanism of regulation, and thus may serve as critical integrators of metabolic and epigenetic signals (Cai et al., 2011; Langer et al., 2002).

The proposed metabolic regulation of KAT activity by CoA led us to consider whether other endogenous inhibitors of these enzymes may exist. Cells contain a diverse repertoire of acyl-CoAs (i.e. malonyl-, succinyl-, butyryl-, propionyl-, crotonyl-, and palmitoyl-CoA). Due to their function as key intermediates in different bioenergetic pathways, the concentration of these molecules directly reflects the metabolic state of the cell. Notably, while diverse lysine acylations have been characterized (Lin et al., 2012), no KAT enzyme has yet been discovered that can utilize these ''alternative'' acyl-CoA cofactors at rates comparable with that of acetyl-CoA. In contrast, extended CoA analogs capable of making high-affinity bisubstrate interactions with KATs are well known as inhibitors of acetylation (Lau et al., 2000). Therefore, we hypothesized that metabolic acyl-CoAs may serve as endogenous bisubstrate inhibitors of KAT enzymes (Figure 1). Metabolic modulation of KAT activity by acyl-CoAs may provide cells with a mechanism to integrate changes in metabolic state and histone acetylation, and potentially fine-tune gene expression under conditions of nutrient stress.

To investigate this hypothesis, here we describe a chemical proteomic approach to define acyl-CoA/KAT interactions in complex proteomes. This approach enables the rapid, direct, and quantitative study of acyl-CoA/KAT interactions in their native contexts, is applicable to multiple KAT family members,

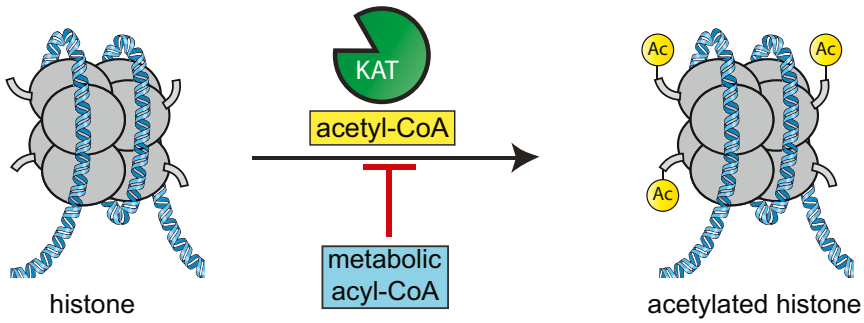

Figure 1. Metabolic Regulation of Histone Lysine Acetyltransferase Activity by Endogenous Acyl-CoAs

By antagonizing acetyl-CoA binding, metabolic acyl-CoAs may inhibit lysine acetyltransferase (KAT) activity, thereby transducing information about the metabolic state of the cell to changes in histone acetylation.

and does not require reconstitution. Applying this approach, we identified a previously unreported palmitoyl-CoA/KAT interaction. Biochemical profiling reveals palmitoyl-CoA and other fatty acyl-CoAs can inhibit KAT activity, with different KAT subfamilies displaying distinct in vitro sensitivities to this inhibition. Adding a palmitoyl-CoA precursor to cells or overexpressing fatty acyl-CoA biosynthetic enzymes reduces cellular histone acetylation. These studies suggest that fatty acyl-CoAs may constitute a novel class of endogenous KAT inhibitors, and propose novel strategies for the metabolic modulation of KAT activity.

RESULTS

A Sensitive Chemical Proteomic Method to Assess KAT Active Site Occupancy

A major challenge to studying the metabolic regulation of KAT activity is that their biologically relevant forms are multiprotein complexes that are difficult to reconstitute in vitro (Roth et al., 2001). Testing whether a metabolite interacts strongly with one or more of these KAT complexes is thus a non-trivial task. To address this challenge, we developed a chemoproteomic approach to study the active site occupancy of intact, multiprotein KAT complexes. This strategy uses an enrichable active site probe to detect catalytically competent KATs directly from cell proteomes (Figure 2). To enable the study of the metabolically sensitive KAT enzymes Gcn5 and pCAF, the probe "core" incorporates H3K14-CoA, a known high-affinity inhibitor of these two enzymes (Lau et al., 2000). For our affinity purification element we introduced a straightforward N-terminal biotin, designed to enable copurification and identification of KAT complex members, and increase the sensitivity of KAT detection by circumventing potentially low-yielding photocrosslinking steps (Montgomery et al., 2014).

In pilot studies, HeLa cell proteomes incubated with H3K14-CoA-biotin **1** (10 μM) were subjected to streptavidin-enrichment and a mild wash step. Liquid chromatography-tandem mass spectrometry (LC-MS/MS) analysis revealed enrichment of Gcn5, as well as several members of its associated multiprotein STAGA complex (Figure 2; Table S1). We also detected enrichment of Mof, a member of the MYST KAT family, including several proteins associated with its NSL complex. Interestingly, copurification of members of other Mof-containing complexes (MSL and MLL) was not observed. For both KAT complexes, enrichment was competed by addition of an active site directed ligand (Figure 2). This indicates that probe **1** is capable of profiling the active site occupancy of KATs within their endogenous multiprotein complexes, and represents a major leap in sensitivity over our previous efforts (Montgomery et al., 2014). In addition to Gcn5, the human GCN5 KAT family contains another member, pCAF, which is 97.8% identical in the KAT catalytic domain but is present at comparably lower levels in HeLa cell extracts. Theoretically pCAF should be amenable to active site directed enrichment by probe **1**, but was not observed in our LC-MS/MS datasets. To test whether immunoblotting could enable the active site mediated analysis of low-abundance KATs not observable by LC-MS/MS, we subjected unfractionated HeLa cell lysates to a single round of affinity enrichment by **1**, followed by immunoblotting with an anti-pCAF antibody. Indeed, we found pCAF was enriched by probe **1**, in a manner that was sensitive to active site competition. This likely reflects the signal amplification afforded by chemiluminescent detection strategies, and highlights immunoaffinity profiling as an ideal approach for the targeted quantification of KAT active site engagement.

Competitive Chemical Proteomic Profiling of Acyl-CoA/KAT Interactions

We next assessed whether probe **1** could be applied in a competitive chemoproteomic approach to study the metabolic sensitivity of native, cellular KAT enzymes (Leung et al., 2003). In this experiment, blockade of KAT active sites by a competing acyl-CoA metabolite results in reduced enrichment of cellular KATs (Gcn5, pCAF, or Mof), impeding their subsequent detection (Figure 3). Thus, in parallel, HeLa cell lysates were incubated with a variety of CoA metabolites (CoA, acetyl-CoA, propionyl-CoA, butyryl-CoA, malonyl-CoA, succinyl-CoA, crotonyl-CoA, and palmitoyl-CoA; Figure S1A), followed by H3K14-CoA-biotin **1** enrichment and anti-KAT immunoblotting.

We observed an overall trend of metabolic acyl-CoAs inhibiting pulldown of Mof > Gcn5 > pCAF (Figure 3). Since **1** likely binds to these three KATs with differing affinities, it is logical that each KAT may display different intrinsic sensitivities to competition in this experiment. Therefore, we focused our analysis on the quantitative rank order trends of metabolite binding to a single KAT, rather than absolute magnitude of competition between different KAT family members. The positive control acetyl-CoA efficiently blocked enrichment of all three KATs, consistent with its known strong interaction with these enzymes (Figure 3). Competitive chemoproteomic analysis demonstrated that the feedback inhibitor CoA also interacted strongly with all three active sites, and was one of the strongest metabolic inhibitors tested. Interestingly, Gcn5 and pCAF interacted more strongly with their feedback inhibitor (CoA) than their cofactor

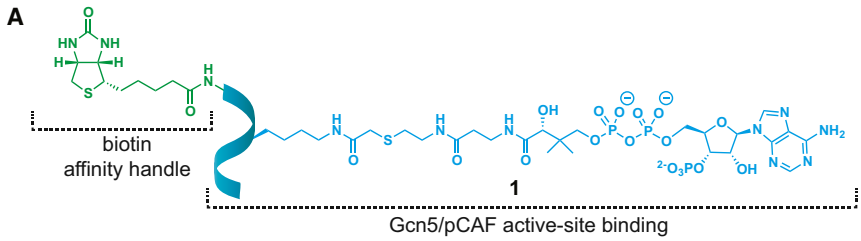

B

	Protein	gene	probe	probe + comp.
Gcn5 STAGA/PCAF complexes	Histone acetyltransferase KAT2A	KAT2A	8	0
	Transformation/transcription domain-associated protein	TRRAP	7	0
	SAGA-associated factor 29 homolog	CCDC101	5	0
	TAF6-like RNA polymerase II 65 kDa subunit 6L	TAF6L	5	0
	Transcriptional adapter 3	TADA3	4	0
	TAF5-like RNA polymerase II 65 kDa subunit 5L	TAF5L	4	0
	Transcription initiation factor TFIID subunit 9B	TAF9B	3	0
	Transcriptional adapter 1	TADA1	3	0
	Transcriptional adapter 2-beta	TADA2B	2	0
MOF NSL complex	Histone acetyltransferase KAT8	KAT8	8	0
	KAT8 regulatory NSL complex subunit 1	KANSL1	7	0
	Microspherule protein 1	MCRS1	4	0
	PHD finger protein 20	PHF20	1	0
	Host cell factor 1	HCFC1	1	0
	KAT8 regulatory NSL complex subunit 3	KANSL3	1	0

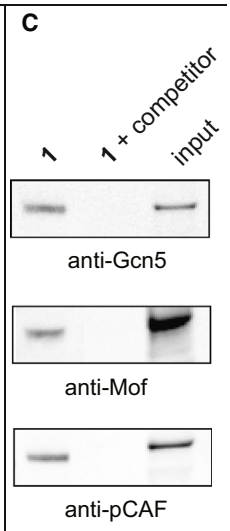

Figure 2. A Chemical Proteomic Strategy for Profiling Cellular KAT Complexes

(A) Schematic of KAT chemical proteomic probe (H3K14-CoA-biotin, 1) used in this study, with ribbon representing H3 peptide. Full structure of probe and competitor are provided in the Supplemental Information.

(B) Spectral counts for KATs and complex members enriched by **1**.

(C) Immunoaffinity profiling of Gcn5, pCAF, and Mof demonstrate active site dependent enrichment of each KAT. Input represents the KAT immunoblot signal from non-enriched control, and competitor refers to the active site directed ligand H3K14-CoA.

(acetyl-CoA), a finding that was distinct from Mof (Figure 3). This provides further evidence that GCN5 family members may be particularly sensitive to changes in the acetyl-CoA/CoA ratio, as has been previously proposed (Albaugh et al., 2011; Cai et al., 2011; Lee et al., 2014; Wellen et al., 2009).

Next, we shifted our focus to investigating whether any metabolic acyl-CoAs are capable of interacting strongly with KATs, potentially indicating their ability to serve as alternative cofactors or endogenous inhibitors of these enzymes. Propionyl- and butyryl-CoA are known to be able to function as alternative cofactors for Gcn5 and pCAF (Leemhuis et al., 2008; Montgomery et al., 2014), and strongly competed for their proteomic enrichment. Mof also interacted strongly with these C3/C4 acyl-CoAs, and propionyl-CoA antagonized Mof enrichment to a similar degree as its natural substrate acetyl-CoA. The ability of propionyl-CoA to function as a cofactor or inhibitor of Mof has not been reported (Chen et al., 2007). Malonyl-, crotonyl-, and succinyl-CoA did not interact strongly with Gcn5 or pCAF (<50% inhibition of pulldown), while Mof was observed to interact weakly with malonyl-CoA. However, we found that palmitoyl-CoA competitively inhibited enrichment of all three KAT enzymes (>50% inhibition of pulldown; Figure 3). Relative to acetyl-CoA, palmitoyl-CoA most strongly antagonized Gcn5 pulldown, followed by Mof and pCAF. In addition to these KAT catalytic domains, palmitoyl-CoA also antagonized enrichment of the STAGA/PCAF component TRRAP (Figure S1B). This indicates that palmitoyl-CoA is able to block the interaction of H3K14-CoA-biotin **1** with a multiprotein KAT complex, presumably by directly competing for the enzyme active site. Control experiments showed that palmitoyl-CoA was not significantly hydrolyzed during these experiments (Figure S2), suggesting that competition was due to palmitoyl-CoA itself and not a downstream effector or by-product. Gcn5, pCAF, and Mof are all known to inefficiently utilize extended acyl-CoA analogs (Chen et al., 2007; Yang et al., 2013), and our own studies provided no evidence that these KATs were capable of using palmitoyl-CoA as a substrate (vide infra). These observations, coupled with the potential significance of a link between transcriptional regulation and fatty acid metabolism, led us to further investigate palmitoyl-CoA as a potentially novel, endogenous KAT inhibitor.

Biochemical Analysis of Fatty Acyl-CoA/KAT Interactions

While the inhibition of KAT activity by palmitoyl-CoA has not been previously reported, fatty acyl-CoAs and fatty acyl-CoA binding proteins have been found in the nuclei of eukaryotic cells (Elholm et al., 2000; Huang et al., 2004; Ves-Losada and Brenner, 1996). Furthermore, these species have been proposed to regulate the activity of transcription factors (Hertz et al., 1998), kinases, and metabolic enzymes (Jenkins et al., 2011; Yang et al., 2005). To extend these observations to KATs, we first used a known crystal structure of the metabolically sensitive KAT Gcn5 to model the human palmitoyl-CoA/Gcn5 complex (Figure 4A) (Poux et al., 2002). The natural cofactor acetyl-CoA binds Gcn5 via hydrogen bonds between the oxygen atoms of the pyrophosphate moiety and the backbone amide nitrogens of Val587, Lys588, Gly589, Thr592, and Lys624, as well as between the phosphopantetheine arm and backbone amides of Cys579 and Val581. Docking suggests that palmitoyl-CoA has the capacity to make identical interactions with the Gcn5 cofactor binding site, potentially anchoring the fatty acyl chain and allowing it to make additional interactions with hydrophobic surfaces in the substrate binding site, similar to synthetic bisubstrate inhibitors (Figure 4A).

To biochemically characterize the effect of palmitoyl-CoA on KAT activity, we applied a coupled-enzyme assay to monitor histone peptide acetylation. To directly compare chemoproteomic and in vitro biochemical methods, we analyzed metabolic acyl-CoAs for inhibition of Gcn5 at a single concentration

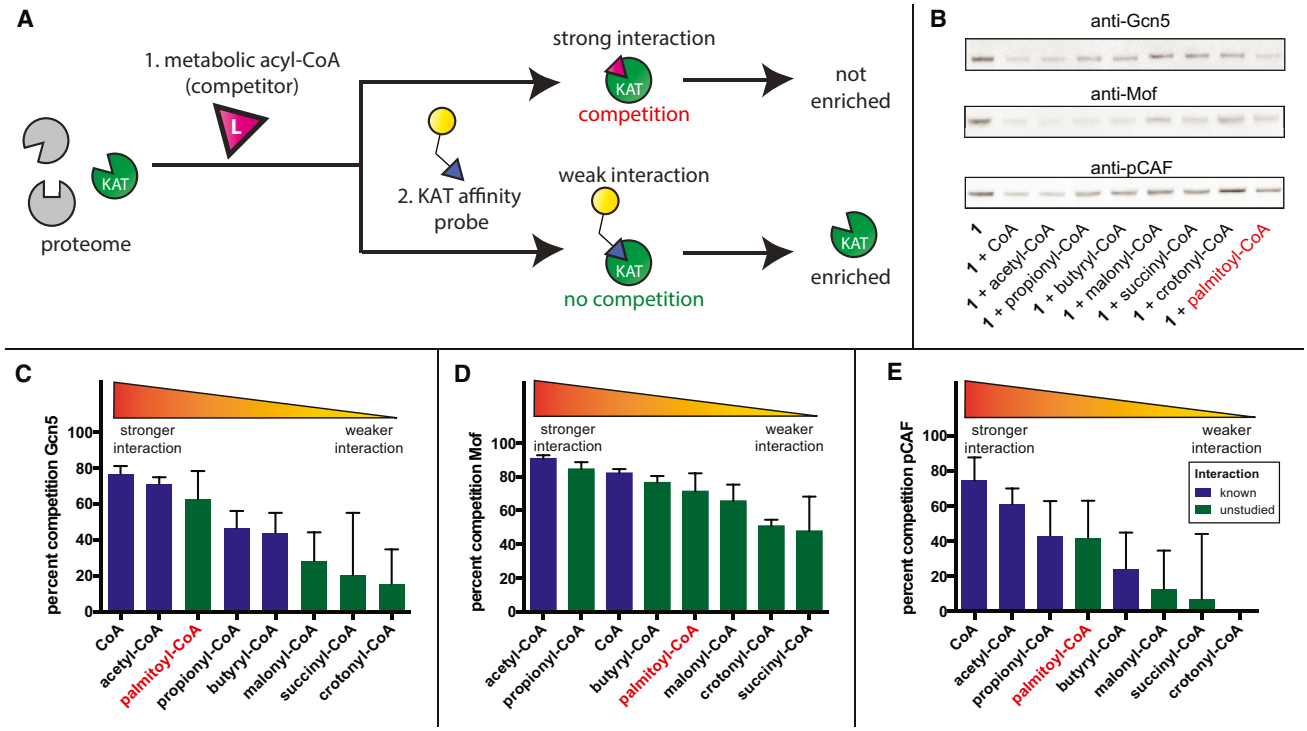

Figure 3. Competitive Chemical Proteomic Profiling of Acyl-CoA/KAT Interactions

(A) Schematic depiction of strategy.

(B) Representative immunoblots depicting enrichment of Gcn5, Mof, and pCAF by probe **1** (10 μM) in the absence or presence of metabolic acyl-CoA competitors (30 μM).

(C–E) Quantitative rank ordering of acyl-CoA interactions with Gcn5 (C), Mof (D), and pCAF (E), as analyzed via gel densitometry. Values represent the average ± SD of three replicates, with percent competition calculated by comparing KAT pulldown in the presence and absence of each acyl-CoA.

(20 μM). Consistent with our chemoproteomic analysis, significant differences ($p < 0.05$) were seen between palmitoyl-CoA and the weak interactors crotonyl-, malonyl-, and succinyl-CoA (Figure S3). No turnover was observed in the absence of acetyl-CoA, indicating that palmitoyl-CoA is not used by Gcn5 as a substrate. Further analysis revealed that palmitoyl-CoA potently inhibits recombinant Gcn5 (K_i = 630 ± 80 nM) at levels far below its critical micellar concentration (~70 μM) (Constantinides and Steim, 1985). Palmitoyl-CoA inhibition best fit a model that was competitive with regard to acetyl-CoA (Figure 4B). Furthermore, free palmitic acid did not affect Gcn5 activity (Figure S4), demonstrating that the C16 fatty acid must be covalently anchored to CoA to mediate its inhibitory effect. To evaluate specificity, we studied the effects of palmitoyl-CoA on the prototypical KAT p300. Palmitoyl-CoA inhibits p300-catalyzed acetylation, although less potently than Gcn5 (K_i = 8,750 ± 1,900 nM). Furthermore, we benchmarked the inhibitory potency of palmitoyl-CoA against desulfo-CoA, a desulfurized CoA analog that has previously been used to study feedback inhibition of Gcn5 and is compatible with KAT coupled-enzyme assays (Tanner et al., 2000b). Desulfo-CoA inhibited Gcn5 less potently than palmitoyl-CoA (K_i = 1,220 ± 190 nM), highlighting palmitoyl-CoA as one of the most potent endogenous KAT-inhibiting metabolites identified to date.

To confirm these results and better understand the structural requirements for KAT inhibition, we next screened CoA, palmitoyl-CoA, and related fatty acyl-CoAs for their effect on Gcn5 activity using an orthogonal, separation-based assay (Fanslau et al., 2010). This assay monitors the ability of KATs to acetylate a fluorescent peptide substrate, which can be separated from non-acetylated peptides in a charged field and thus provide a direct and quantitative readout of KAT activity. While not amenable to the determination of biochemical inhibition constants, this assay does enable the direct comparison of the inhibitory potency of CoA and palmitoyl-CoA (CoA itself is technically incompatible with the coupled-enzyme method). Separation-based analyses of KAT activity confirmed that palmitoyl-CoA inhibited Gcn5 more potently than CoA (66% versus 29% inhibition at 10 μM, respectively). Expansion of this method to analyze a fatty acyl-CoA panel found Gcn5 was inhibited more potently by C18 fatty acyl-CoAs (linoleoyl- and oleoyl-CoA) than C14/C16 (Figure 4C). Beyond these differences in magnitude of inhibition, the larger general trend observed was that all fatty acyl-CoAs, regardless of chain length or unsaturation, had the net effect of inhibiting KAT activity (Figure 4C). The high number of rotatable bonds in palmitoyl-CoA limits rigorous computational treatment, and a definitive model of palmitoyl-CoA/Gcn5 binding will require structural analyses. However, docking studies support the finding that Gcn5 can bind a variety of fatty acyl-CoAs, as the majority of contacts of the fatty acyl chain are made generically with hydrophobic surfaces in the shallow substrate binding groove of the enzyme rather than in a deep,

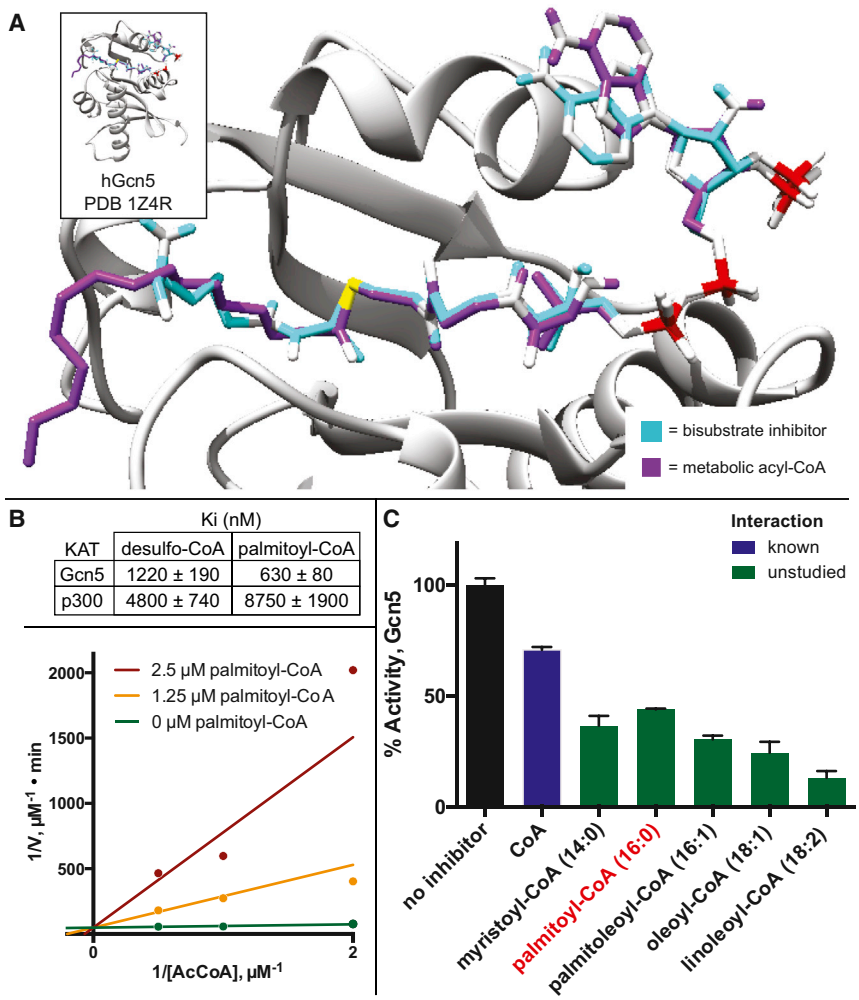

Figure 4. Biochemical Characterization of Fatty Acyl-CoA/KAT Interactions

(A) Homology model of human Gcn5 bound to bisubstrate inhibitor H3K14-CoA and palmitoyl-CoA.

(B) Analysis of metabolic inhibition of Gcn5 via coupled-enzyme assay Lineweaver-Burk plot depicting acetyl-CoA competitive inhibition of Gcn5 by palmitoyl-CoA.

(C) Analysis of metabolic inhibition of Gcn5 via separation-based assay. Palmitoyl-CoA and related fatty acyl-CoAs inhibit Gcn5 biochemical activity more potently than CoA. Structures of fatty acyl-CoAs are provided in Figure S1.

specific binding pocket (Figure 4A). The ability of Gcn5 to promiscuously interact with fatty acyl-CoAs is similar to the broad-spectrum binding exhibited by fatty acid binding transcription factors (Lin et al., 1999). These data also suggest that overall cellular fatty acyl-CoA content, rather than any individual fatty acyl-CoA signal, may be the most important determinant for inhibition of cellular KAT activity by this mechanism.

Modulating Fatty Acyl-CoA Biosynthesis Can Affect Histone Acetylation in Cells

Determining whether fatty acyl-CoAs can act as endogenous inhibitors of KATs in cells is challenging due to many factors, including the lack of cell permeability of these molecules, the central role of fatty acyl-CoAs to many cell processes, and the difficulty of quantifying subcellular fatty acyl-CoA concentrations. Indeed, the overall nuclear/cytosolic concentration of fatty acyl-CoAs, which our biochemical analyses indicate may be a key regulator of KAT activity, has not been quantitatively determined for any cell line. Nevertheless, the inhibition constants measured here are lower than the K_m values that many long-chain acyl-CoA metabolizing enzymes exhibit for palmitoyl-CoA (~1 μM) (Powell et al., 1985), and fatty acyl-CoA concentrations in the micromolar range have been demonstrated to modulate the activity of many proteins including glucokinase (Tippett and Neet, 1982), protein kinase C (Majumdar et al., 1991), carnitine palmitoyltransferase (Agius et al., 1987), and the nuclear thyroid hormone receptor (Li et al., 1990). This suggests that the observed inhibition of KATs by fatty acyl-CoAs may be biologically relevant, and led us to investigate the relationship between fatty acyl-CoA biosynthesis and histone acetylation in cells.

As already mentioned, fatty acyl-CoAs are not directly cell permeable. Therefore, we first evaluated the effect of palmitate, a palmitoyl-CoA precursor, on cellular histone acetylation. In HEK293T cells, we found that supplementation of media with palmitate (0.1 mM) led to a slight, but measurable, decrease in several histone marks, including H3K9Ac, H3K14Ac, H3K27Ac, and H4K8Ac (Figure 5). However, this effect is small, and could be due to either stimulation of fatty acyl-CoA/KAT interactions or KAT-independent, off-target effects. Thus, to further implicate fatty acyl-CoAs directly as inhibitors of histone acetylation, we tested how manipulation of palmitoyl-CoA biosynthesis affected this process. Palmitate is activated to palmitoyl-CoA by the activity of ATP-dependent, long-chain acyl-CoA synthetase (ACSL) enzymes (Figure 5). The human genome encodes five ACSL family members, and related medium-chain acyl-CoA synthetases are known to possess considerable overlap in their ability to activate palmitate (Watkins et al., 2007). Therefore, we employed a gain-of-function approach to test whether overexpression of a fatty acyl-CoA biosynthetic enzyme further antagonized acetylation. As many ACSL enzymes are membrane proteins, we chose an ACSL family member (ACSL3) known to express partial nuclear membrane localization as a potential candidate for the production of nuclear fatty acyl-CoAs (Poppelreuther et al., 2012). ACSL3 was cloned with a C-terminal FLAG tag into a mammalian expression vector under control of a constitutive CMV promoter. Transient transfection and overexpression of FLAG-ACSL3 in HEK293T cells prominently reduced histone acetylation. H3K9 and H3K14 are known targets of GCN5 family KATs (Jin et al., 2011), and

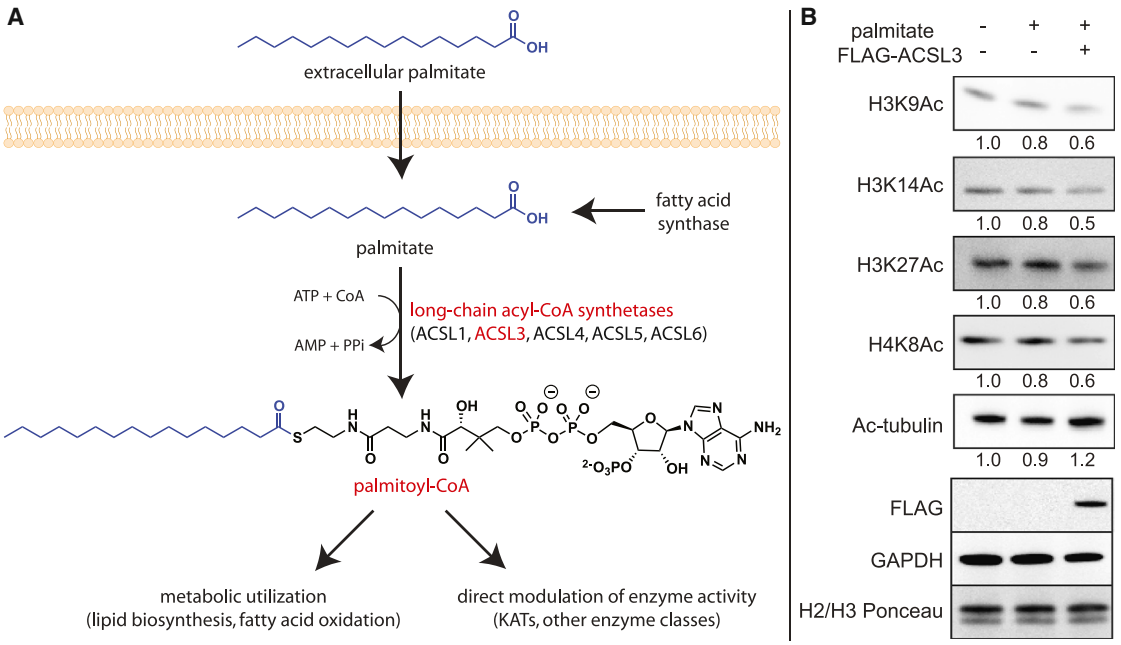

Figure 5. Cellular Effects of Palmitoyl-CoA Precursors and Palmitoyl-CoA Synthetases on Histone Acetylation

(A) Long-chain acyl-CoA synthetase (ACSL)-dependent formation of palmitoyl-CoA from palmitate.

(B) (Top) Effect of palmitate treatment and ACSL3 overexpression on histone acetylation in HEK293T cells. Values under each immunoblot represent the densitometry quantified band intensity relative to the control (lane 1). All quantified values were normalized based on Ponceau staining to account for differences in loading between different lanes (Figure S5A). (Bottom) Cytosolic/nuclear loading controls and verification of FLAG-ACLS3 overexpression.

acetylation of each of these residues was strongly reduced. H4K8 and H3K27, which are not Gcn5-regulated targets, were also antagonized. However, acetylation of the cytoskeletal protein tubulin was not affected (Figure 5). Interestingly, overexpression of ACSL3 alone (without palmitate supplementation) was also found to inhibit histone acetylation, suggesting that endogenous fatty acids may be mobilized to stimulate deacetylation in an ACSL-dependent manner (Figure S5B).

We emphasize that these results must be interpreted with caution, as ACSL3 overexpression may have effects on metabolism and enzyme activity that facilitate KAT-independent mechanisms of deacetylation and will require further analysis to dissect. In particular, the KDAC enzyme SIRT6 has been shown to be biochemically activated by long-chain fatty acids (although this enzyme primarily acts on H3K9Ac/H3K56Ac substrates, and thus would not explain the observed inhibition of H4 acetylation) (Feldman et al., 2013). However, the strong stimulation of deacetylation by fatty acyl-CoA biosynthetic enzymes, together with our biochemical analyses, are consistent with the hypothesis that fatty acyl-CoAs may be capable of metabolically facilitating cellular deacetylation programs by functioning as endogenous inhibitors of KAT enzymes.

DISCUSSION

The discovery that chromatin-mediated signaling cascades are sensitive to the metabolic state of the cell has the potential to powerfully illuminate the etiology of cancer and also inspire new therapeutic strategies. However, a major challenge lies in identifying direct mechanistic links between metabolites and specific chromatin modifiers. Here, we have applied a novel competitive chemoproteomic approach to identify a metabolic-epigenetic interaction that potentially links tumor hypoacetylation and altered lipid metabolism on a molecular level (Nomura et al., 2010; Seligson et al., 2005). Palmitoyl-CoA is capable of interacting with KATs in the context of their multiprotein complexes and can potently inhibit their catalytic activity at concentrations <1 μM, making it one of the most potent metabolic inhibitors of KAT activity characterized to date. Previous studies have identified fatty acyl-CoA and fatty acyl-CoA binding proteins in the nucleus (Elholm et al., 2000; Ves-Losada and Brenner, 1996), and micromolar concentrations of palmitoyl-CoA have been implicated in the regulation of many cellular proteins, including transcription factors (Hertz et al., 1998). While the literature and data are compelling, a relevant question is whether fatty acyl-CoAs are able to accumulate in cells to concentrations sufficient to affect KAT activity. One possibility is that fatty acyl-CoAs may be supplied to KATs at high local concentrations by fatty acyl-CoA binding proteins, as has been proposed for other fatty acyl-CoA regulated enzymes (Elholm et al., 2000). Alternatively, the finding that a wide range of fatty acyl-CoAs can inhibit KATs suggests the potential for overall fatty acyl-CoA concentrations to reach levels sufficient to affect KAT activity.

While the subcellular concentrations (i.e. nuclear/cytosolic versus mitochondrial) of fatty acyl-CoAs have never been quantitatively characterized, studies in rats have observed that several abundant fatty acyl-CoAs are upregulated under conditions of nutrient stress, such as fasting (Woldegiorgis et al., 1985). Wellen and coworkers have previously drawn a direct correlation between bioenergetic stress, reduced acetyl-CoA/CoA

ratio, and inhibition of histone acetylation (Lee et al., 2014; Wellen et al., 2009). Our findings extend this paradigm, and suggest that in some cases this phenomenon may be mediated by additional metabolic factors such as palmitoyl-CoA. Interestingly, a recent study observed that cells grown in galactose-palmitate exhibit both increased fatty acid oxidation and greatly reduced histone acetylation, relative to cells grown on traditional high-glucose media (Pougovkina et al., 2014). Since fatty acid oxidation requires transient synthesis of nuclear/cytosolic fatty acyl-CoA, it is intriguing to speculate that direct inhibition of KATs by endogenous fatty acyl-CoAs may play a role in this process, possibly facilitating gene-expression programs that aid adaptation to conditions of bioenergetic stress.

Finally, beyond the potential biological ramifications of these findings, our results also suggest a solution to a long-standing challenge in acetylation biology: how to deliver potent KAT-inhibiting bisubstrate inhibitors to cells. Our studies imply that metabolic acyl-CoAs are capable of inhibiting KAT-catalyzed acetylation with some degree of selectivity. It is therefore intriguing to speculate that this mechanism may be exploited to manipulate the concentrations of metabolic acyl-CoAs, thereby producing endogenous KAT bisubstrate inhibitors in cells. Notably, a wide array of metabolites and xenobiotics are known to be activated to CoA analogs via the activity of acyl-CoA synthetase enzymes (Darnell and Weidolf, 2013). Defining the tissue-specific production and interaction of these metabolic acyl-CoAs with KATs may provide a new paradigm for the targeted regulation of KAT activity. Such studies will require improved tools for the rapid development of KAT-metabolite interactions, as the human genome encodes at least 30 enzymes that have demonstrated evidence of KAT activity, only three of which were analyzed with the chemical proteomic approach reported here. In the future, we envision that improved chemical proteomic approaches will enable the generation of global KAT cofactor affinity maps (Becher et al., 2013), providing novel insights into the metabolic regulation of KAT activity and strategic manipulation of acetylation-dependent signaling in disease.

SIGNIFICANCE

Recent studies have found that many chromatin-mediated signaling cascades are regulated by the metabolic state of the cell. One mechanism by which metabolism can affect epigenetic signaling is through the production of endogenous inhibitors of chromatin-modifying enzymes. Here, we have developed a chemical proteomic strategy to enable the identification of new endogenous inhibitors of KAT enzymes. These studies led to the identification of palmitoyl-CoA, a metabolite whose KAT inhibitory properties have been heretofore unstudied, as a potentially novel endogenous inhibitor of KAT activity. Palmitoyl-CoA and related fatty acyl-CoAs potently inhibit the prototypical KAT Gcn5, and cell culture studies suggest (but do not conclusively demonstrate) that this mechanism may be operable in cells. These studies highlight the utility of chemical proteomic methods to rapidly characterize metabolic-epigenetic interactions, and propose that metabolic manipulation of endogenous inhibitors may be a viable strategy for modulating KAT activity in vivo.

EXPERIMENTAL PROCEDURES

Compounds, Enzymes, and Materials

Recombinant p300 (1,195–1,662) and Gcn5 (497–662) were obtained from Enzo. Acetyl-CoA, propionyl-CoA, butyryl-CoA, succinyl-CoA, crotonyl-CoA, malonyl-CoA, and palmitoyl-CoA were synthesized according to published procedures (Padmakumar et al., 1997). All synthesized CoA analogs were purified by high-performance liquid chromatography, with purity verified by LC-MS prior to use. Linoleoyl-CoA, myristoyl-CoA, oleoyl-CoA, and palmitoleoyl-CoA were purchased from Sigma with purity verified by LC-MS prior to use. H3K14-CoA and desulfo-CoA were synthesized according to previously reported procedures (Chase et al., 1966; Montgomery et al., 2014; Zheng et al., 2004). Qubit Protein Assay kit (Life Technologies) was used to determine cell lysate and histone extract concentrations. Pyruvate dehydrogenase (PDH), ketoglutarate dehydrogenase, and nicotinamide adenine dinucleotide were purchased from Sigma. Lab-Chip EZ-Reader 12-sipper chip (#760404) and ProfilerPro Separation Buffer (#760367) were purchased from Perkin-Elmer. H3K9Ac (9649P), H3K14Ac (7627P), H3K27Ac (8173), H4K8Ac (2594P), acetylated tubulin (5225P), glyceraldehyde-3-phosphate dehydrogenase (5174S), Gcn5 (3305S), and pCAF (3378S) antibodies were purchased from Cell Signaling Technologies, while Mof (A300-992A-T) antibody was purchased from Bethyl Laboratories.

Chemical Proteomic Analysis of KAT/Acyl-CoA Interactions

For each analysis, 50 μl of streptavidin-agarose resin (prewashed with 3 × 1 ml of PBS) was incubated with 10 μM H3K14-CoA-biotin (**1**) in 500 μl of PBS and rotated for 1 hr at room temperature. Whole-cell lysates were clarified via filtration (EMD-Millipore, SLGV033RS), adjusted to a final protein concentration of 1.5 mg/ml, and split into 500 μl (0.75 mg) aliquots. For competitive samples, the metabolic acyl-CoA or cognate competitor (H3K14-CoA) was preincubated with lysate for 30 min on ice. Following equilibration, beads were pelleted by centrifugation (1400 rcf, 3 min) and the supernatant was removed, before addition of the corresponding lysate sample. Samples were rotated for 1 hr at room temperature, and pelleted by centrifugation (1400 rcf, 3 min). After removal of lysate solution, beads were washed with ice-cold buffer (50 mM Tris-HCl [pH 7.5], 5% glycerol, 1.5 mM $MgCl_2$, 150 mM NaCl, 3 × 500 μl) and collected in centrifugal filters (VWR, 82031-256). For western blot analysis, samples were eluted in 1× SDS sample buffer (95°C, 2 × 10 min). For proteomic analysis, 400 μl of trypsin buffer (50 mM Tris-HCl [pH 8.0], 1 M urea) was added to each sample, followed by 0.4 μl of 1 M $CaCl_2$ and 4 μl of trypsin (0.25 mg/ml), and digests were allowed to proceed overnight at 37°C. After extraction, tryptic peptide samples were acidified to a final concentration of 5% formic acid and frozen at −80°C for LC-MS/MS analysis.

Continuous Assay for Lysine Peptide Acetylation: Coupled-Enzyme Assay

KAT activity was measured by a continuous coupled-enzyme assay (Kim et al., 2000). In this assay, CoA produced by KAT-catalyzed acetylation is used by PDH to produce the reduced form of NAD^+ (NADH), which can be monitored spectrophotometrically at 340 nm. Assays were performed in 150-μl volumes containing 50 mM Bis-Tris, 50 mM Tris, 100 mM sodium acetate (TBA buffer, pH 7.5), 5 mM $MgCl_2$, 1 mM DTT, 2.4 mM pyruvate, 200 μM thiamine pyrophosphate, 200 μM NAD^+, and 0.035 units of PDH (as defined by supplier), unlabeled histone peptide (H3 5–20 for Gcn5, H4 3–14 for p300; 60 μM), and 150 nM Gcn5 or 100 nM p300. Reactions were plated in 96-well plates and allowed to equilibrate at room temperature for 10 min. Reactions were initiated by addition of acetyl-CoA and analyzed continuously for 5 min by measuring NADH production at 340 nm. Initial velocities were determined by linear regression and background corrected by subtracting the rate of spontaneous formation of CoA (determined from reactions lacking Gcn5/p300). Kinetic parameters (K_m and V_{max}) for acetyl-CoA, and inhibition constants (K_i) for palmitoyl- and desulfo-CoA were determined by holding the concentration of substrate peptide constant (H3 5–20 for Gcn5, H4 3–14 for p300; 60 μM) and initiating reactions with acetyl-CoA (4.1–33.3 μM) in the presence or absence of inhibitor (0–20 μM). All calculations were performed using Graphpad Prism 6. Michaelis-Menten parameters for acetyl-CoA were calculated by non-linear regression of initial velocities. Kinetic parameters for acetyl-CoA were used to appropriately constrain non-linear regression analyses of

inhibitor data. Data were fit to equations for competitive, non-competitive, or uncompetitive inhibition and assessed for global goodness of fit (R^2 values) to determine the optimal mode of inhibition. The inhibition constant K_i for each inhibitor was computed by using equations $K_{m(obs)} = K_m \times (1 + [I]/K_i)$ and $Y = V_{max} \times X/(K_{m(obs)} + X)$, where X is substrate concentration, Y is response, [I] is the concentration of inhibitor, V_{max} is the maximum response in the absence of inhibitor (expressed in the same units as Y), and K_m is the Michaelis-Menten constant (expressed in the same units as X). Reported values are based on competitive model of inhibition.

Separation-Based Assay for Lysine Peptide Acetylation: Microfluidic Mobility Shift

Gcn5 activity was also measured using an orthogonal separation-based assay (Fanslau et al., 2010). This method detects acetylation of a fluorescein isothiocyanate (FITC)-labeled Gcn5 substrate peptide (histone H3; FITC-Ahx-QTARKSTGGKAPRKQL) based on its altered electrophoretic mobility relative to non-acetylated peptide. Assays were performed in 30 μl of reaction buffer (50 mM HEPES [pH 7.5], 50 mM NaCl, 2 mM EDTA, 2 mM DTT, 0.05% Triton X-100) with KAT (GCN5 [100 nM], p300 [50 nM]) and FITC-peptide (FITC-H3 for GCN5; FITC-H4 for p300). Reactions were plated in 384-well plates, allowed to equilibrate at room temperature for 10 min, and initiated by addition of acetyl-CoA (final concentration 0.63–10 μM). Reactions were monitored in real time following transfer to a Lab-Chip EZ-Reader at ambient temperature and analyzed by microfluidic electrophoresis. Optimized separation conditions were: downstream voltage −500 V, upstream voltage −2,500 V, and a pressure of −1.5 psi for FITC-H3 5–20 and FITC-H4 3–14. Percent conversion was calculated by ratiometric measurement of substrate/product peak heights. Percent activity represents the relative acetylation in inhibitor-treated reactions relative to untreated control, measured in triplicate, and corrected for non-enzymatic acetylation.

Docking Studies of Palmitoyl-CoA/Gcn5 Complex

The crystal structures of the KAT catalytic domain of human Gcn5 (PDB: 1Z4R) and H3K14-CoA ligand (PDB: 1M1D) were retrieved from the PDB for use in the docking calculations (Schuetz et al., 2007). The Protein Preparation Wizard of the Schrödinger suite was used to prepare the binding site of Gcn5. The protein was processed by assigning bond orders, adding hydrogens, removing cocrystallized water molecules, and creating disulfide bonds. Finally, a restrained minimization with a root-mean-square deviation of 0.30 was applied using the OPLS 2005 force field to optimize the hydrogen bond network. Docking studies were performed using Glide (version 5.8; Schrödinger). The prepared Gcn5 structure was employed to generate the receptor energy grid centered on the cocrystallized ligand. The extra-precision (XP) docking protocol was used. Palmitoyl-CoA has 38 rotatable bonds, which means the configuration space for docking poses is enormous. To facilitate the sampling of the ligand conformations, we therefore set up a core constraint for the flexible docking in Glide. This core constraint was defined using the heavy atoms of the cofactor moiety of the cocrystallized ligand from PDB structure 1Z4R. The docking poses obtained in this way were then redocked again, but this time without constraints, using the refine mode in Glide.

Cellular Analyses of Histone Acetylation

HEK293T cells were cultured in DMEM supplemented with 10% fetal bovine serum and L-glutamine (2 mM). For histone acetylation analyses, HEK293T cells were plated in six-well dishes (6×10^5 cells/well) and allowed to adhere for 24 hr. At this point, transfections were performed using Lipofectamine 3000 (7.5 μl/well; Life Technologies) and plasmid DNA (2,500 ng) according to the manufacturer's protocol. After 6 hr the medium was removed, cells were washed with PBS, and fresh medium was added containing either palmitate-conjugated BSA (100 μM palmitate) or BSA control. Cells were incubated with or without palmitate for 24 hr and harvested for histone extraction. Following removal of media, cells were washed once with PBS and incubated with 300 μl of Triton extraction buffer (TEB; PBS with 0.5% Triton X-100, 2 mM PMSF, and 0.02% NaN_3), harvested by gentle lifting, and transferred to microcentrifuge tubes. Samples were incubated in TEB for 30 min on ice, pelleted at 6,500 relative centrifugal force (rcf) for 10 min at 4°C, and the supernatant removed and saved for cytosolic protein analysis. Nuclei were resuspended, washed again with TEB (150 μl), and pelleted at 6,500 rcf for 10 min at 4°C. For acid extraction of histones, each pellet was treated with 0.4 N H_2SO_4 (75 μl) and rotated overnight at 4°C. Samples were centrifuged at 11,000 rcf for 10 min at 4°C, and histones were precipitated from the supernatant by addition of 20% TCA (750 μl). After at least 1 hr, samples were centrifuged at 16,000 rcf for 10 min at 4°C, and the pellets were washed with acetone/0.1% HCl (750 μl) and neat acetone (750 μl), with centrifugations at 16,000 rcf for 10 min at 4°C following each wash. Samples were air-dried at room temperature, dissolved in ddH_2O, and quantified by Qubit Protein Assay kit (Life Technologies). Samples were prepared for western blot analysis using Bis-Tris NuPAGE gels (12%) and MES running buffer in Xcell SureLock MiniCells (Invitrogen) according to the manufacturer's instructions. Following antibody incubation and washing, antibody binding was detected using LumiGLO (Cell Signaling Technologies) and chemiluminescent signal visualized using an ImageQuant Las4010 Digitial Imaging System (GE Healthcare). Immunoblot signals were quantified using ImageQuant TL software (GE Healthcare).

SUPPLEMENTAL INFORMATION

Supplemental Information includes Supplemental Experimental Procedures, five figures, one table, and scheme and procedure for synthesis and analytical data for H3K14-CoA-biotin and can be found with this article online at http://dx.doi.org/10.1016/j.chembiol.2015.06.015.

AUTHOR CONTRIBUTIONS

D.C.M., A.W.S., and J.L.M. designed experiments. D.C.M. performed all chemical proteomic and cell-based experiments. A.W.S. performed biochemical experiments and analyses and assisted with cell-based experiments. M.C.N. and L.G. performed modeling analysis. D.C.M., A.W.S., and J.L.M. analyzed data and wrote the manuscript.

ACKNOWLEDGMENTS

The authors thank Dr. Ming Zhou (Laboratory of Proteomics and Analytical Technology) for LC-MS/MS analyses and Dr. Carissa Grose (Protein Expression Laboratory) for assisting with cloning and preparation of plasmid DNA. Cellular extracts were prepared from HeLa cells grown by the National Cell Culture Center (NCCC, Minneapolis, MN). This work was supported by the Intramural Research Program of the NIH, National Cancer Institute, Center for Cancer Research (ZIA BC011488-02).

Received: May 12, 2015
Revised: June 4, 2015
Accepted: June 5, 2015
Published: July 16, 2015

REFERENCES

Agius, L., Wright, P.D., and Alberti, K.G. (1987). Carnitine acyltransferases and acyl-CoA hydrolases in human and rat liver. Clin. Sci. (Lond.) *73*, 3–10.

Albaugh, B.N., Arnold, K.M., and Denu, J.M. (2011). KAT(ching) metabolism by the tail: insight into the links between lysine acetyltransferases and metabolism. ChemBioChem *12*, 290–298.

Becher, I., Savitski, M.M., Savitski, M.F., Hopf, C., Bantscheff, M., and Drewes, G. (2013). Affinity profiling of the cellular kinome for the nucleotide cofactors ATP, ADP, and GTP. ACS Chem. Biol. *8*, 599–607.

Cai, L., Sutter, B.M., Li, B., and Tu, B.P. (2011). Acetyl-CoA induces cell growth and proliferation by promoting the acetylation of histones at growth genes. Mol. Cell *42*, 426–437.

Chase, J.F., Middleton, B., and Tubbs, P.K. (1966). A coenzyme A analogue, desulpho-coA; preparation and effects on various enzymes. Biochem. Biophys. Res. Commun. *23*, 208–213.

Chen, Y., Sprung, R., Tang, Y., Ball, H., Sangras, B., Kim, S.C., Falck, J.R., Peng, J., Gu, W., and Zhao, Y. (2007). Lysine propionylation and butyrylation are novel post-translational modifications in histones. Mol. Cell. Proteomics *6*, 812–819.

Comerford, S.A., Huang, Z., Du, X., Wang, Y., Cai, L., Witkiewicz, A.K., Walters, H., Tantawy, M.N., Fu, A., Manning, H.C., et al. (2014). Acetate dependence of tumors. Cell *159*, 1591–1602.

Constantinides, P.P., and Steim, J.M. (1985). Physical properties of fatty acyl-CoA. Critical micelle concentrations and micellar size and shape. J. Biol. Chem. *260*, 7573–7580.

Darnell, M., and Weidolf, L. (2013). Metabolism of xenobiotic carboxylic acids: focus on coenzyme A conjugation, reactivity, and interference with lipid metabolism. Chem. Res. Toxicol. *26*, 1139–1155.

Dhalluin, C., Carlson, J.E., Zeng, L., He, C., Aggarwal, A.K., and Zhou, M.M. (1999). Structure and ligand of a histone acetyltransferase bromodomain. Nature *399*, 491–496.

Donohoe, D.R., Collins, L.B., Wali, A., Bigler, R., Sun, W., and Bultman, S.J. (2012). The Warburg effect dictates the mechanism of butyrate-mediated histone acetylation and cell proliferation. Mol. Cell *48*, 612–626.

Elholm, M., Garras, A., Neve, S., Tornehave, D., Lund, T.B., Skorve, J., Flatmark, T., Kristiansen, K., and Berge, R.K. (2000). Long-chain acyl-CoA esters and acyl-CoA binding protein are present in the nucleus of rat liver cells. J. Lipid Res. *41*, 538–545.

Fanslau, C., Pedicord, D., Nagulapalli, S., Gray, H., Pang, S., Jayaraman, L., Lippy, J., and Blat, Y. (2010). An electrophoretic mobility shift assay for the identification and kinetic analysis of acetyl transferase inhibitors. Anal. Biochem. *402*, 65–68.

Feldman, J.L., Baeza, J., and Denu, J.M. (2013). Activation of the protein deacetylase SIRT6 by long-chain fatty acids and widespread deacylation by mammalian sirtuins. J. Biol. Chem. *288*, 31350–31356.

Hertz, R., Magenheim, J., Berman, I., and Bar-Tana, J. (1998). Fatty acyl-CoA thioesters are ligands of hepatic nuclear factor-4alpha. Nature *392*, 512–516.

Huang, H., Starodub, O., McIntosh, A., Atshaves, B.P., Woldegiorgis, G., Kier, A.B., and Schroeder, F. (2004). Liver fatty acid-binding protein colocalizes with peroxisome proliferator activated receptor alpha and enhances ligand distribution to nuclei of living cells. Biochemistry *43*, 2484–2500.

Jenkins, C.M., Yang, J., Sims, H.F., and Gross, R.W. (2011). Reversible high affinity inhibition of phosphofructokinase-1 by acyl-CoA: a mechanism integrating glycolytic flux with lipid metabolism. J. Biol. Chem. *286*, 11937–11950.

Jin, Q., Yu, L.R., Wang, L., Zhang, Z., Kasper, L.H., Lee, J.E., Wang, C., Brindle, P.K., Dent, S.Y., and Ge, K. (2011). Distinct roles of GCN5/PCAF-mediated H3K9ac and CBP/p300-mediated H3K18/27ac in nuclear receptor transactivation. EMBO J. *30*, 249–262.

Kim, Y., Tanner, K.G., and Denu, J.M. (2000). A continuous, nonradioactive assay for histone acetyltransferases. Anal. Biochem. *280*, 308–314.

Langer, M.R., Fry, C.J., Peterson, C.L., and Denu, J.M. (2002). Modulating acetyl-CoA binding in the GCN5 family of histone acetyltransferases. J. Biol. Chem. *277*, 27337–27344.

Lau, O.D., Kundu, T.K., Soccio, R.E., Ait-Si-Ali, S., Khalil, E.M., Vassilev, A., Wolffe, A.P., Nakatani, Y., Roeder, R.G., and Cole, P.A. (2000). HATs off: selective synthetic inhibitors of the histone acetyltransferases p300 and PCAF. Mol. Cell *5*, 589–595.

Lee, J.V., Carrer, A., Shah, S., Snyder, N.W., Wei, S., Venneti, S., Worth, A.J., Yuan, Z.F., Lim, H.W., Liu, S., et al. (2014). Akt-dependent metabolic reprogramming regulates tumor cell histone acetylation. Cell Metab. *20*, 306–319.

Leemhuis, H., Packman, L.C., Nightingale, K.P., and Hollfelder, F. (2008). The human histone acetyltransferase P/CAF is a promiscuous histone propionyltransferase. ChemBioChem *9*, 499–503.

Leung, D., Hardouin, C., Boger, D.L., and Cravatt, B.F. (2003). Discovering potent and selective reversible inhibitors of enzymes in complex proteomes. Nat. Biotechnol. *21*, 687–691.

Li, Q.L., Yamamoto, N., Inoue, A., and Morisawa, S. (1990). Fatty acyl-CoAs are potent inhibitors of the nuclear thyroid hormone receptor in vitro. J. Biochem. *107*, 699–702.

Lin, Q., Ruuska, S.E., Shaw, N.S., Dong, D., and Noy, N. (1999). Ligand selectivity of the peroxisome proliferator-activated receptor alpha. Biochemistry *38*, 185–190.

Lin, H., Su, X., and He, B. (2012). Protein lysine acylation and cysteine succination by intermediates of energy metabolism. ACS Chem. Biol. *7*, 947–960.

Majumdar, S., Rossi, M.W., Fujiki, T., Phillips, W.A., Disa, S., Queen, C.F., Johnston, R.B., Jr., Rosen, O.M., Corkey, B.E., and Korchak, H.M. (1991). Protein kinase C isotypes and signaling in neutrophils. Differential substrate specificities of a translocatable calcium- and phospholipid-dependent beta-protein kinase C and a phospholipid-dependent protein kinase which is inhibited by long chain fatty acyl coenzyme A. J. Biol. Chem. *266*, 9285–9294.

Marks, P.A., and Breslow, R. (2007). Dimethyl sulfoxide to vorinostat: development of this histone deacetylase inhibitor as an anticancer drug. Nat. Biotechnol. *25*, 84–90.

Meier, J.L. (2013). Metabolic mechanisms of epigenetic regulation. ACS Chem. Biol. *8*, 2607–2621.

Montgomery, D.C., Sorum, A.W., and Meier, J.L. (2014). Chemoproteomic profiling of lysine acetyltransferases highlights an expanded landscape of catalytic acetylation. J. Am. Chem. Soc. *136*, 8669–8676.

Nomura, D.K., Long, J.Z., Niessen, S., Hoover, H.S., Ng, S.W., and Cravatt, B.F. (2010). Monoacylglycerol lipase regulates a fatty acid network that promotes cancer pathogenesis. Cell *140*, 49–61.

Padmakumar, R., Padmakumar, R., and Banerjee, R. (1997). Large-scale synthesis of coenzyme A esters. Methods Enzymol. *279*, 220–224.

Poppelreuther, M., Rudolph, B., Du, C., Grossmann, R., Becker, M., Thiele, C., Ehehalt, R., and Fullekrug, J. (2012). The N-terminal region of acyl-CoA synthetase 3 is essential for both the localization on lipid droplets and the function in fatty acid uptake. J. Lipid Res. *53*, 888–900.

Pougovkina, O., te Brinke, H., Ofman, R., van Cruchten, A.G., Kulik, W., Wanders, R.J., Houten, S.M., and de Boer, V.C. (2014). Mitochondrial protein acetylation is driven by acetyl-CoA from fatty acid oxidation. Hum. Mol. Genet. *23*, 3513–3522.

Poux, A.N., Cebrat, M., Kim, C.M., Cole, P.A., and Marmorstein, R. (2002). Structure of the GCN5 histone acetyltransferase bound to a bisubstrate inhibitor. Proc. Natl. Acad. Sci. USA *99*, 14065–14070.

Powell, G.L., Tippett, P.S., Kiorpes, T.C., Mcmillinwood, J., Coll, K.E., Schulz, H., Tanaka, K., Kang, E.S., and Shrago, E. (1985). Fatty acyl-CoA as an effector molecule in metabolism. Fed. Proc. *44*, 81–84.

Roth, S.Y., Denu, J.M., and Allis, C.D. (2001). Histone acetyltransferases. Annu. Rev. Biochem. *70*, 81–120.

Schuetz, A., Bernstein, G., Dong, A., Antoshenko, T., Wu, H., Loppnau, P., Bochkarev, A., and Plotnikov, A.N. (2007). Crystal structure of a binary complex between human GCN5 histone acetyltransferase domain and acetyl coenzyme A. Proteins *68*, 403–407.

Seligson, D.B., Horvath, S., Shi, T., Yu, H., Tze, S., Grunstein, M., and Kurdistani, S.K. (2005). Global histone modification patterns predict risk of prostate cancer recurrence. Nature *435*, 1262–1266.

Seligson, D.B., Horvath, S., McBrian, M.A., Mah, V., Yu, H., Tze, S., Wang, Q., Chia, D., Goodglick, L., and Kurdistani, S.K. (2009). Global levels of histone modifications predict prognosis in different cancers. Am. J. Pathol. *174*, 1619–1628.

Shimazu, T., Hirschey, M.D., Newman, J., He, W., Shirakawa, K., Le Moan, N., Grueter, C.A., Lim, H., Saunders, L.R., Stevens, R.D., et al. (2013). Suppression of oxidative stress by beta-hydroxybutyrate, an endogenous histone deacetylase inhibitor. Science *339*, 211–214.

Tanner, K.G., Langer, M.R., and Denu, J.M. (2000a). Kinetic mechanism of human histone acetyltransferase P/CAF. Biochemistry *39*, 11961–11969.

Tanner, K.G., Langer, M.R., Kim, Y., and Denu, J.M. (2000b). Kinetic mechanism of the histone acetyltransferase GCN5 from yeast. J. Biol. Chem. *275*, 22048–22055.

Thompson, P.R., Kurooka, H., Nakatani, Y., and Cole, P.A. (2001). Transcriptional coactivator protein p300. Kinetic characterization of its histone acetyltransferase activity. J. Biol. Chem. *276*, 33721–33729.

Tippett, P.S., and Neet, K.E. (1982). Specific inhibition of glucokinase by long-chain acyl co-enzymes A below the critical micelle concentration. J. Biol. Chem. *257*, 2839–2845.

Ves-Losada, A., and Brenner, R.R. (1996). Long-chain fatty Acyl-CoA synthetase enzymatic activity in rat liver cell nuclei. Mol. Cell. Biochem. *159*, 1–6.

Watkins, P.A., Maiguel, D., Jia, Z., and Pevsner, J. (2007). Evidence for 26 distinct acyl-coenzyme A synthetase genes in the human genome. J. Lipid Res. *48*, 2736–2750.

Wellen, K.E., Hatzivassiliou, G., Sachdeva, U.M., Bui, T.V., Cross, J.R., and Thompson, C.B. (2009). ATP-citrate lyase links cellular metabolism to histone acetylation. Science *324*, 1076–1080.

Woldegiorgis, G., Spennetta, T., Corkey, B.E., Williamson, J.R., and Shrago, E. (1985). Extraction of tissue long-chain acyl-CoA esters and measurement by reverse-phase high-performance liquid chromatography. Anal. Biochem. *150*, 8–12.

Yang, J., Gibson, B., Snider, J., Jenkins, C.M., Han, X., and Gross, R.W. (2005). Submicromolar concentrations of palmitoyl-CoA specifically thioesterify cysteine 244 in glyceraldehyde-3-phosphate dehydrogenase inhibiting enzyme activity: a novel mechanism potentially underlying fatty acid induced insulin resistance. Biochemistry *44*, 11903–11912.

Yang, C., Mi, J., Feng, Y., Ngo, L., Gao, T., Yan, L., and Zheng, Y.G. (2013). Labeling lysine acetyltransferase substrates with engineered enzymes and functionalized cofactor surrogates. J. Am. Chem. Soc. *135*, 7791–7794.

Zheng, Y., Thompson, P.R., Cebrat, M., Wang, L., Devlin, M.K., Alani, R.M., and Cole, P.A. (2004). Selective HAT inhibitors as mechanistic tools for protein acetylation. Methods Enzymol. *376*, 188–199.